Electronic Supplementary Information

Enhancing the thermally activated delayed fluorescence of *nido*-carborane-appended triarylboranes by steric modification of the phenylene linker

Surendran Sujith,[a] Eun Bi Nam,[b] Junseong Lee,[c] Sang Uck Lee*[b] and Min Hyung Lee*[a]

[a]Department of Chemistry, University of Ulsan, Ulsan 44610, Republic of Korea
[b]Department of Bionano Technology and Department of Applied Chemistry, Hanyang University, Ansan 15588, Republic of Korea
[c]Department of Chemistry, Chonnam National University, Gwangju 61186, Republic of Korea

1. Experimental

1.1. General considerations

All operations were performed under an inert nitrogen atmosphere using standard Schlenk and glove box techniques. Anhydrous grade solvents (Aldrich) were dried over activated molecular sieves (5Å). Spectrophotometric-grade THF (Merck) was used for photophysical measurements. Commercial reagents were used without further purification after purchase. Deuterated solvents from Cambridge Isotope Laboratories were used. NMR spectra were recorded on a Bruker AM 300 (300.13 MHz for ^{1}H, 75.48 MHz for ^{13}C, 96.29 MHz for ^{11}B) or a Bruker AVANCE III HD 400 (400.13 MHz for ^{1}H, 100.61 MHz for ^{13}C) spectrometer at ambient temperature. Chemical shifts (in ppm) are referenced against external Me_4Si (^{1}H, ^{13}C) and $BF_3{\cdot}OEt_2$ (^{11}B). Elemental analyses were performed on a Flash 2000 elemental analyzer (Thermo Scientific) by the Research Facilities Center at University of Ulsan. Melting points (mp) were measured by Melting Point Apparatus SMP30 (Stuart Equipment). Cyclic voltammetry experiments were carried out using an Autolab/PGSTAT101 system.

1.2. Synthesis

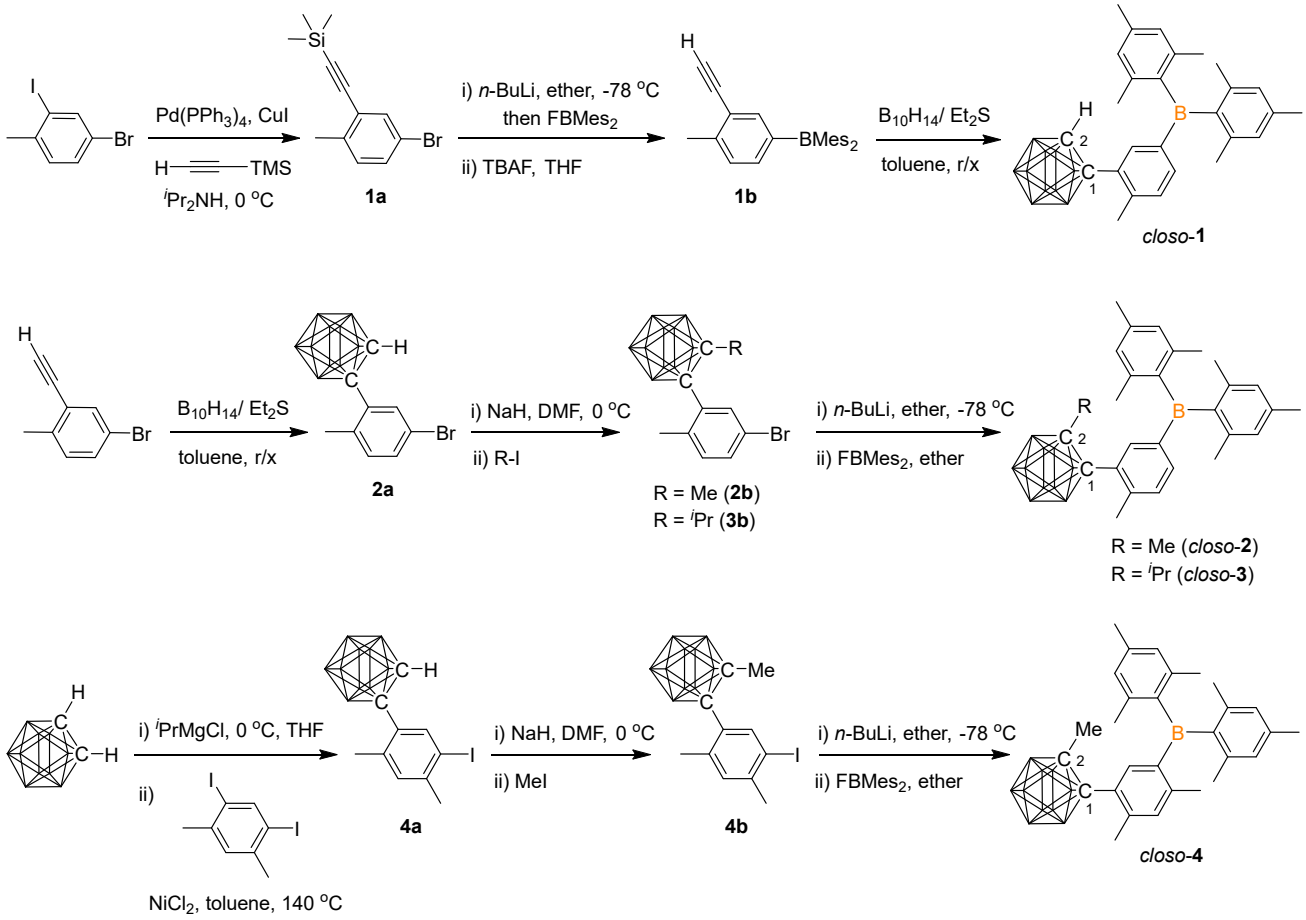

Scheme S1. Synthesis of *closo*-carborane-appended triarylboranes, *closo*-**1**–**4**.

((5-Bromo-2-methylphenyl)ethynyl)trimethylsilane (1a)

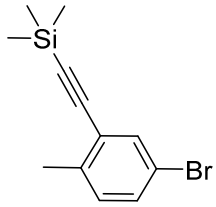

4-Bromo-2-iodo-1-methylbenzene (3.0 g, 10.1 mmol), CuI (0.09 g, 0.5 mmol), and $Pd(PPh_3)_4$ (0.58 g, 0.5 mmol) were dissolved in anhydrous diisopropylamine (*i*-Pr_2NH) (30 mL). Into the solution was added trimethylsilylacetylene (1.42 mL, 10.1 mmol), and the reaction mixture was stirred at 60 °C for 20 h. The resulting solution was evaporated off under reduced pressure and the crude product was extracted with diethyl ether (40 mL × 3). After evaporation of solvent, the solid residue was purified by column chromatography on silica gel using hexane as eluent. Drying *in vacuo* afforded a white powder of **1a** (2.33 g, 86%). ^{1}H NMR ($CDCl_3$): δ 7.58 (d, J = 2.1 Hz, 1H), 7.34 (dd, J = 9.0, 3.0 Hz, 1H), 7.07 (d, J = 9.0 Hz, 1H), 2.39 (s, 3H), 0.28 (s, 9H). ^{13}C NMR ($CDCl_3$): δ 139.6, 134.7, 131.5, 130.9, 125.0, 118.6, 102.5, 100.0, 20.4, 0.0.

(3-Ethynyl-4-methylphenyl)dimesitylborane (1b)

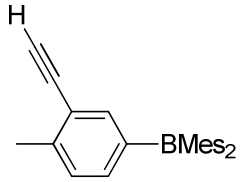

To a solution of **1a** (0.77 g, 2.89 mmol) in THF (10 mL) was added *n*-BuLi (2.5 M in hexane, 1.38 mL, 3.4 mmol) at −78 °C, and the mixture was stirred for 1 h at this temperature. A solution of dimesitylboron fluoride ($FBMes_2$, 0.852 g, 3.17 mmol) in THF (4 mL) was then added. After stirring for 1 h, the reaction mixture was slowly allowed to reach room temperature and was stirred overnight. Removal of the solvent under reduced pressure produced a sticky residue, which was subjected to column chromatography on silica gel using hexane to afford ((5-(dimesitylboryl)-2-methylphenyl)ethynyl)trimethylsilane as a white powder (0.71 g, 56%). ^{1}H NMR ($CDCl_3$): δ 7.65 (d, J = 1.1 Hz, 1H), 7.37 (dd, J = 7.6, 1.3 Hz, 1H), 7.21 (d, J = 7.6 Hz, 1H), 6.84 (s, 4H), 2.51 (s, 3H), 2.34 (s, 6H), 2.01 (s, 12H), 0.27 (s, 9H). Next, this compound (0.71 g, 1.62 mmol) was dissolved in anhydrous THF (30 mL) and tetra-*n*-butylammonium fluoride (*n*-Bu_4NF, TBAF) solution (1.0 M in THF, 1.9 mL) was added under nitrogen atmosphere. After stirring at room temperature for 3 h, the resulting solution was evaporated off under reduced pressure. The crude product was extracted with diethyl ether (40 mL × 3). After evaporation of solvent, the solid residue was purified by column chromatography on silica gel using hexane as eluent. Drying *in vacuo* afforded a white powder of **1c** (0.54 g, 94%). ^{1}H NMR

($CDCl_3$): δ 7.67 (d, J = 1.2 Hz, 1H), 7.41 (dd, J = 7.6, 1.3 Hz, 1H), 7.22 (d, J = 7.6 Hz, 1H), 6.84 (s, 4H), 3.25 (s, 1H), 2.53 (s, 3H), 2.33 (s, 6H), 2.02 (s, 12H).^{13}C NMR ($CDCl_3$): δ 145.1, 143.2, 141.5, 140.9, 140.6, 138.8, 136.9, 129.4, 128.4, 121.9, 82.8, 81.1, 23.6, 21.4, 21.1.

1-(Mes_2B)-3-(2-H-*o*-carboran-1-yl)-4-methylbenzene (*closo*-1)

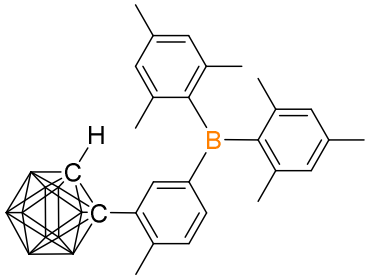

A toluene solution (20 mL) of decaborane ($B_{10}H_{14}$, 0.22 g, 1.80 mmol) and diethyl sulfide (Et_2S, 0.87 mL, 8.9 mmol) was stirred at room temperature for 0.5 h and then **1b** (0.54 g, 1.48 mmol) in toluene (10 mL) was slowly added to this solution. The mixture was refluxed for 4 days under nitrogen atmosphere. After cooling down to room temperature, the solvent was evaporated off under reduced pressure and the residue was purified by column chromatography on silica gel using hexane as eluent, giving *closo*-**1** as a white powder (0.16 g, 22%). ^{1}H NMR ($CDCl_3$): δ 7.68 (s, 1H), 7.42 (d, J = 7.6 Hz, 1H), 7.15 (d, J = 7.6 Hz, 1H), 6.89 (s, 4H), 4.43 (s, 1H), 2.67 (s, 3H), 2.36 (s, 6H), 2.03 (s, 12H). ^{13}C NMR ($CDCl_3$): δ 144.0, 141.1, 140.8, 139.3, 139.2, 139.1, 137.1, 133.8, 131.6, 128.5, 78.2, 59.9, 23.7, 23.6, 21.4. ^{11}B NMR ($CDCl_3$): δ 75.9 (br s), 1.1 (1B), −3.3 (2B), −9.0 (7B). mp = 180 °C. Anal. Calcd for $C_{27}H_{39}B_{11}$: C, 67.21; H, 8.15%. Found: C, 67.20; H, 8.12%.

1-Bromo-3-(2-H-*o*-carboran-1-yl)-4-methylbenzene (2a)

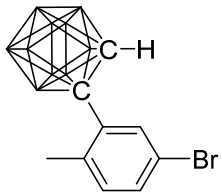

A toluene solution (20 mL) of decaborane ($B_{10}H_{14}$, 1.18 g, 9.65 mmol) and diethyl sulfide (Et_2S, 4.06 mL, 40.3 mmol) was stirred at room temperature for 0.5 h. Into the solution was added a toluene solution (10 mL) of 4-bromo-2-ethynyl-1-methylbenzene (1.57 g, 8.06 mmol), which was obtained from desilylation of **1a** using TBAF in THF. The mixture was refluxed for 4 days under nitrogen atmosphere. Work-up and purification of the crude product by column chromatography on silica gel using hexane as eluent afforded **2a** as a white powder (0.61 g, 24%). ^{1}H NMR ($CDCl_3$): δ 7.70 (d, J = 1.8 Hz, 1H), 7.39 (dd, J = 8.1, 1.8 Hz, 1H), 7.02 (d, J = 8.4 Hz, 1H), 4.55 (s, 1H), 3.4–1.0 (br, 10H, B–*H*), 2.53 (s, 3H).

^{13}C NMR ($CDCl_3$): δ 135.4, 134.0, 133.9, 133.7, 132.5, 120.5, 76.8, 59.), 22.9. ^{11}B NMR ($CDCl_3$): δ −1.8 (2B), −8.6 (3B), −10.8 (5B).

1-Bromo-3-(2-Me-*o*-carboran-1-yl)-4-methyl benzene (2b)

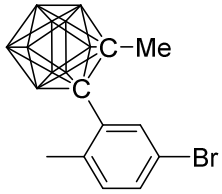

Sodium hydride (NaH, 60% dispersion in mineral oil, 0.06 g, 1.43 mmol) was suspended in dry DMF (5 mL). After cooling down to 0 °C, a solution of **2a** (0.30 g, 0.96 mmol) in DMF (5 mL) was added slowly to the suspension. The mixture was stirred at 0 °C for 1 h, and then MeI (0.18 mL, 2.08 mmol) was added. After stirring at room temperature overnight, the reaction was quenched by addition of saturated aqueous NH_4Cl solution, and the mixture was extracted with diethyl ether (20 mL × 3). The organic layer was washed with water (20 mL × 3), separated, and dried over $MgSO_4$. The solvent was evaporated under reduced pressure and the residue was purified by column chromatography on silica gel using hexane as eluent. Drying *in vacuo* afforded a white powder of **2b** (0.23 g, 74%). ^{1}H NMR ($CDCl_3$): δ 8.01 (d, J = 1.8 Hz, 1H), 7.47 (dd, J = 8.1, 1.8 Hz, 1H), 7.14 (d, J = 8.1 Hz, 1H), 2.68 (s, 3H), 3.4–1.0 (br, 10H, B–*H*), 1.74 (s, 3H). ^{13}C NMR ($CDCl_3$): δ 139.0, 137.4, 135.9, 133.5, 130.6, 120.1, 82.8, 79.5, 23.8, 23.6. ^{11}B NMR ($CDCl_3$): δ −1.8 (1B), −3.4 (1B), −8.5 (2B), −10.9 (6B).

1-(Mes_2B)-3-(2-Me-*o*-carboran-1-yl)-4-methylbenzene (*closo*-2)

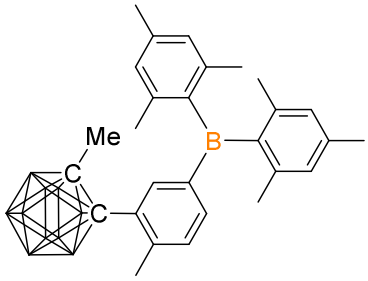

To a solution of **2b** (0.20 g, 0.61 mmol) in THF (10 mL) was added a hexane solution of *n*-BuLi (2.5 M, 0.26 mL, 0.67 mmol) at −78 °C, and the mixture was stirred for 1 h at this temperature. A solution of dimesitylboron fluoride (0.18 g, 0.67 mmol) in THF (4 mL) was then added. After stirring for 1 h, the reaction mixture was slowly allowed to warm to room temperature and was stirred overnight. Work-up and purification of the crude product by column chromatography afforded a white powder of *closo*-**2** (0.18 g, 61%). ^{1}H NMR ($CDCl_3$): δ 7.98 (s, 1H), 7.46 (d, J = 7.6 Hz, 1H), 7.24 (d, J = 7.6 Hz, 1H), 6.86 (s, 4H), 2.78 (s, 3H), 2.35 (s, 6H), 2.00 (s, 12H), 1.65 (s, 3H). ^{13}C NMR ($CDCl_3$) δ 144.0, 143.2, 141.9,

141.2, 140.7, 139.2, 137.8, 134.3, 128.5, 128.4, 84.3, 79.2, 24.5, 23.5, 23.4, 21.4. ^{11}B NMR ($CDCl_3$): δ 77.3 (br s), 1.5 (2B), −3.4 (2B), −8.9 (6B). mp = 172 °C. Anal. Calcd for $C_{28}H_{41}B_{11}$: C, 67.73; H, 8.32%. Found: C, 67.69; H, 8.27%.

1-Bromo-3-(2-*i*-Pr-*o*-carboran-1-yl)-4-methyl benzene (3b)

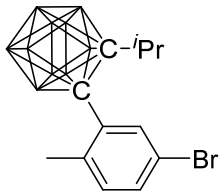

This compound was prepared in a manner analogous to the synthesis of **2b** using **2a** (0.30 g, 0.96 mmol) and *i*-PrI (0.26 g, 2,80 mmol) in DMF (5 mL) to give a white powder of **3b** (0.29 g, 56%). ^{1}H NMR ($CDCl_3$): δ 7.99 (d, J = 1.9 Hz, 1H), 7.47 (dd, J = 8.3, 2.0 Hz, 1H), 7.13 (d, J = 8.3 Hz, 1H), 2.67 (s, 3H), 3.6–1.4 (br, 10H, B–*H*), 1.74 (sept, J = 6.9 Hz, 1H), 1.07 (d, J = 6.9 Hz, 6H). ^{13}C NMR ($CDCl_3$): δ 139.0, 137.5, 135.9, 133.5, 130.5, 120.2, 91.1, 86.2, 32.2, 24.0, 23.6. ^{11}B NMR ($CDCl_3$): δ −4.0 (1B), −6.1 (1B), −11.4 (8B).

1-(Mes_2B)-3-(2-*i*-Pr-*o*-carboran-1-yl)-4-methylbenzene (*closo*-3)

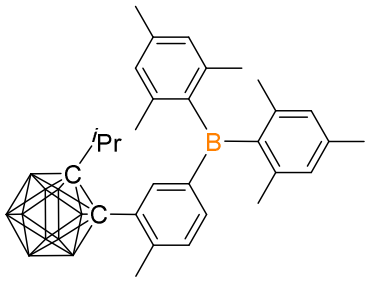

This compound was prepared in a manner analogous to the synthesis of *closo*-**2** using **3b** (0.18 g, 0.51 mmol) to give a white powder of *closo*-**3** (0.15 g, 55%).^{1}H NMR ($CDCl_3$): δ 7.95 (s, 1H), 7.45 (d, J = 7.6 Hz, 1H), 7.23 (d, J = 7.6 Hz, 1H), 6.85 (s, 4H), 2.76 (s, 3H), 2.35 (s, 6H), 1.99 (s, 12H), 1.67 (sept, J = 6.9 Hz, 1H, –C*H*CH_3), 1.00 (d, J = 6.9 Hz, 6H, –CHCH_3). ^{13}C NMR ($CDCl_3$): δ 144.6, 143.9, 143.0, 141.2, 140.7, 139.3, 137.6, 134.3, 128.5, 128.2, 90.9, 88.0, 31.9, 24.3, 23.8, 23.5, 21.4. ^{11}B NMR ($CDCl_3$): δ 77.9 (br s), −3.2 (1B), −4.5 (2B), −10.0 (7B). mp = 154 °C. Anal. Calcd for $C_{30}H_{45}B_{11}$: C, 68.68; H, 8.65%. Found: C, 68.65; H, 8.63%.

1-Iodo-5-(2-H-*o*-carboran-1-yl)-2,4-dimethylbenzene (4a)

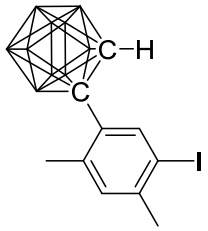

To a THF solution (5 mL) of *o*-carborane (0.29 g, 2.0 mmol) in a pressure vessel was slowly added *i*-PrMgCl (2.0 M in THF, 1.2 mL, 2.4 mmol) at 0 °C, and the mixture was stirred for 1 h. After evaporation of THF, toluene (5 mL), 1,5-diiodo-2,4-dimethylbenzene (0.78 g, 2.2 mmol), and $NiCl_2$ (5.2 mg, 0.04 mmol) were added and the mixture was heated at 140 °C for 36 h. The reaction mixture was then quenched with water (10 mL) and extracted with diethyl ether (20 mL × 3). The combined ether layers were concentrated to dryness under reduced pressure. The crude product was purified by flash column chromatography on silica gel using hexane as eluent to give a white powder of **4a** (0.38 g, 50%). ^{1}H NMR ($CDCl_3$): δ 7.92 (s, 1H), 7.00 (s, 1H), 4.50 (s, 1H), 2.50 (s, 3H), 2.37 (s, 3H). ^{13}C NMR ($CDCl_3$): δ 143.3, 140.9, 135.0, 134.7, 131.1, 98.3, 76.4, 59.8, 27.2, 22.9. ^{11}B NMR ($CDCl_3$): δ −3.0 (3B), −8.3 (7B).

1-Iodo-5-(2-Me-*o*-carboran-1-yl)-2,4-dimethylbenzene (4b)

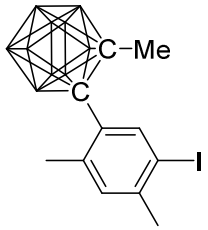

This compound was prepared in a manner analogous to the synthesis of **2b** using **4a** (0.25 g, 0.66 mmol) in DMF (5 mL) to give a white powder of **4b** (0.20 g, 77%). ^{1}H NMR ($CDCl_3$): δ 8.23 (s, 1H), 7.11 (s, 1H), 2.63 (s, 3H), 2.40 (s, 3H), 1.73 (s, 3H). ^{13}C NMR ($CDCl_3$): δ 144.6, 144.4, 139.8, 135.3, 128.0, 98.0, 82.6, 79.4, 27.3, 23.7, 23.5. ^{11}B NMR ($CDCl_3$): δ −3.2 (2B), −9.7 (8B).

1-(Mes_2B)-5-(2-Me-*o*-carboran-1-yl)-2,4-dimethylbenzene (*closo*-4)

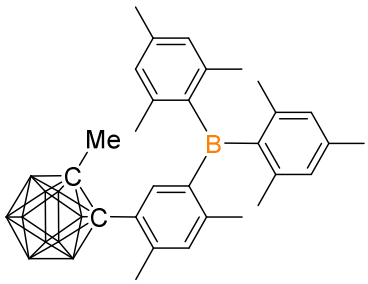

This compound was prepared in a manner analogous to the synthesis of *closo*-**2** using **4b** (0.19 g, 0.49 mmol) to give a white powder of *closo*-**4** (0.14 g, 56%). ^{1}H NMR ($CDCl_3$): δ 7.65 (s, 1H), 7.01 (s, 1H), 6.81 (s, 4H), 2.70 (s, 3H), 2.32 (s, 6H), 2.05 (s, 3H), 1.98 (s, 12H), 1.57 (s, 3H). ^{13}C NMR ($CDCl_3$): δ 146.1, 144.8, 142.6, 142.3, 141.9, 140.2, 139.4, 135.9, 128.6, 125.8, 84.4, 79.2, 23.9, 23.2, 23.1, 21.5, 21.4. ^{11}B NMR ($CDCl_3$): δ 78.0 (br s), −2.1 (1B), −4.4 (1B), −8.9 (3B), −10.9 (4B), −12.6 (1B). mp = 187 °C. Anal. Calcd for $C_{29}H_{43}B_{11}$: C, 68.22; H, 8.49%. Found: C, 68.42; H, 8.25%.

General synthesis of *nido*-carborane-appended triarylboranes, *nido*-1–4

Closo-carborane compounds (0.2 mmol) and *n*-Bu_4NF (TBAF) (1.0 mmol) were dissolved in THF (20 mL) and the mixture was refluxed for 4 d (*nido*-**1**, **2**, **4**) or for 5 d (*nido*-**3**). After cooling down to room temperature, the solvent was evaporated, and the residue was purified by column chromatography on alumina using CH_2Cl_2/hexane (1:1, v/v) followed by acetone as eluent to give a white powder of *nido*-carborane derivatives. The product was further purified by recrystallization from CH_2Cl_2/hexane.

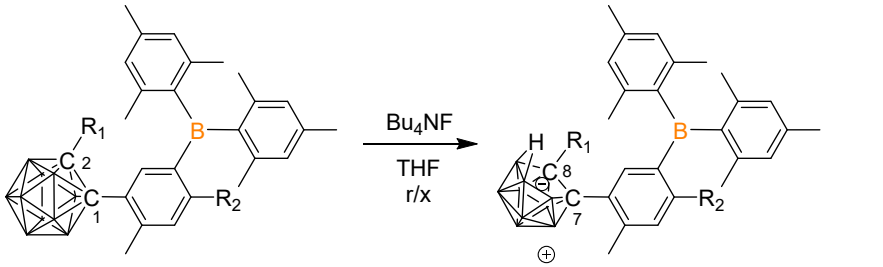

R_1 = H; R_2 = H (*closo*-**1**)
R_1 = Me; R_2 = H (*closo*-**2**)
R_1 = ^{i}Pr; R_2 = H (*closo*-**3**)
R_1 = Me; R_2 = Me (*closo*-**4**)

R_1 = H; R_2 = H (*nido*-**1**)
R_1 = Me; R_2 = H (*nido*-**2**)
R_1 = ^{i}Pr; R_2 = H (*nido*-**3**)
R_1 = Me; R_2 = Me (*nido*-**4**)

Scheme S2. Synthesis of *nido*-carborane-appended triarylboranes, *nido*-**1**–**4**. Reaction time: 4 d for *nido*-**1**, **2**, **4** and 5 d for *nido*-**3**.

[Bu_4N][1-(Mes_2B)-3-(8-H-7,8-*nido*-$C_2B_9H_{10}$)-4-MeC_6H_3] (*nido*-1)

Yield = 64%. ^{1}H NMR (acetone-d_6): δ 7.54 (s, 1H), 7.09–7.03 (m, 2H), 6.79 (s, 4H), 3.5–1.5 (br, 9H, B–*H*), 3.45 (t, J = 9 Hz, 8H), 2.49 (s, 3H), 2.26 (s, 6H), 1.96 (s, 12H), 1.83 (quin, J = 9, 8H), 1.67 (s, 1H, C_{Cb}–*H*),1.43 (sext, J = 7.8, Hz, 8H), 0.98 (t, J = 7.5 Hz, 12H), −2.53 (br s, 1H, B–*H*–B). ^{13}C NMR (acetone-d_6): δ 145.6, 144.2, 142.7, 141.3, 140.2, 139.2, 135.8, 134.0, 129.0, 127.6, 59.3 (Bu_4N), 24.4 (Bu_4N), 24.0, 23.6, 21.2, 20.3 (Bu_4N), 13.9 (Bu_4N) (Cb–*C* signals were not observed). ^{11}B NMR (acetone-d_6): δ 78.1 (br s), −7.9 (2B), −11.0 (1B), −15.7 (1B), −17.8 (3B). −33.1 (1B), −35.6 (1B). mp = 222 °C. Anal. Calcd for $C_{43}H_{75}B_{10}N$: C, 72.32; H, 10.59; N, 1.96%. Found: C, 72.16; H, 10.83, N, 2.01%.

[Bu$_4$N][1-(Mes$_2$B)-3-(8-Me-7,8-*nido*-C$_2$B$_9$H$_{10}$)-4-MeC$_6$H$_3$] (*nido*-2)

Yield = 83%. ^{1}H NMR (acetone-d_6): δ 7.23 (s, 1H), 7.21 (d, J = 1.6 Hz, 1H), 7.10 (d, J = 7.8 Hz, 1H), 3.5–1.5 (br, 9H, B–*H*), 3.45 (t, J = 9 Hz, 8H), 2.40 (s, 3H), 2.28 (s, 6H), 1.98 (s, 12H), 1.84 ((quin, J = 8.1, 8H)), 1.45 (sext, J = 7.5, Hz, 8H), 1.04 (s, 3H, C$_{Cb}$–C*H*$_3$), 0.99 (t, J = 7.3 Hz, 12H), −2.46 (br s, 1H, B–*H*–B). ^{13}C NMR (acetone-d_6): δ 146.1, 143.2, 142.8, 141.2, 139.4, 138.8, 134.6, 129.9, 128.9, 59.4 (Bu$_4$N), 24.4 (Bu$_4$N), 23.7, 23.6, 22.2, 21.2, 20.4 (Bu$_4$N), 13.9 (Bu$_4$N) (Cb–*C* signals were not observed). ^{11}B NMR (acetone-d_6): δ 78.0 (br s), −8.7 (1B), −12.0 (1B), −16.1 (2B), −18.3 (br, 3B), −33.5 (1B), −36.2 (1B). mp = 221 °C. Anal. Calcd for C$_{44}$H$_{77}$B$_{10}$N: C, 72.57; H, 10.66; N, 1.92%. Found: C, 72.18; H, 10.85, N, 2.02%.

[Bu$_4$N][1-(Mes$_2$B)-3-(8-^{i}Pr-7,8-*nido*-C$_2$B$_9$H$_{10}$)-4-MeC$_6$H$_3$] (*nido*-3)

Yield = 59%. ^{1}H NMR (acetone-d_6): δ 7.55 (s, 1H), 7.14–7.08 (m, 2H), 6.80 (s, 4H), 3.50–1.50 (br, 9H, B–*H*), 3.45 (t, J = 8.6 Hz, 8H), 2.60 (s, 3H), 2.27 (s, 6H, Mes–C*H*$_3$), 1.98 (s, 12H, Mes–C*H*$_3$), 1.84 (quin, J = 7.2 8H), 1.44 (sext, J = 7.5 Hz, 8H), 1.25 (sept, J = 6.6 Hz, 1H), 0.99 (t, J = 7.2 Hz, 12H), 0.97 (d, J = 2.1 Hz, 3H), 0.64 (d, J = 6.9 Hz, 3H), −2.60 (br s, 1H, B–*H*–B). ^{13}C NMR (acetone-d_6): δ 146.2, 142.8, 142.6, 141.2, 140.5, 138.8, 134.7, 130.1, 128.9, 59.4 (NBu$_4$), 26.2, 25.3, 24.4 (NBu$_4$), 23.7, 23.6, 21.2, 20.4 (NBu$_4$), 13.8 (NBu$_4$) (Cb–*C* signals were not observed). ^{11}B NMR (acetone-d_6): δ 77.7 (br s), −7.7 (1B), −8.7 (1B), −11.6 (1B), −17.2 (3B), −19.3 (1B), −33.4 (1B), −35.9 (1B). mp = 172 °C. Anal. Calcd for C$_{46}$H$_{81}$B$_{10}$N: C, 73.06; H, 10.80; N, 1.85%. Found: C, 72.86; H, 10.71; N, 1.87%.

[Bu$_4$N][1-(Mes$_2$B)-5-(8-Me-7,8-*nido*-C$_2$B$_9$H$_{10}$)-2,4-Me$_2$C$_6$H$_2$] (*nido*-4)

Yield = 61%. ^{1}H NMR (acetone-d_6): δ 7.23 (s, 1H), 6.87 (s, 1H), 6.76 (s, 4H), 3.5–1.5 (br, 9H, B–*H*), 3.44 (t, J = 8.4 Hz, 8H), 2.44 (s, 3H), 2.25 (s, 6H), 1.96 (s, 3H), 1.95 (s, 12H), 1.83 (quin, J = 8.4, 8H), 1.44 (sext, J = 7.5, Hz, 8H), 1.04 (s, 3H), 0.98 (t, J = 7.5 Hz, 12H), −2.43 (br s, 1H, B–*H*–B).^{13}C NMR (acetone-d_6): δ 144.7, 144.1, 144.0, 140.7, 140.4, 140.1, 138.8, 137.6, 131.8, 128.9, 59.3 (Bu$_4$N), 24.3 (Bu$_4$N), 23.5, 23.2, 21.9, 21.8, 21.2, 20.3 (Bu$_4$N), 13.8 (Bu$_4$N) (Cb–*C* signals were not observed). ^{11}B NMR (acetone-d_6): δ 78.0 (br s), −7.9 (2B), −14.2 (1B), −16.0 (3B), −18.6 (1B), −32.8 (1B), −35.1 (1B). mp = 227 °C. Anal. Calcd for C$_{45}$H$_{79}$B$_{10}$N: C, 72.82; H, 10.73; N, 1.89%. Found: C, 72.79; H, 10.73; N, 1.91%.

[Me$_4$N][1-(Mes$_2$B)-3-(8-H-7,8-*nido*-C$_2$B$_9$H$_{10}$)-4-MeC$_6$H$_3$] (Me$_4$N salt of *nido*-1)

Closo-**1** (70 mg, 0.145 mmol) was added into a solution of KOH (69 mg, 1.16 mmol) in EtOH (8 mL). The mixture was stirred for 1 h at room temperature and then refluxed for 48 h. After cooling the mixture to room temperature, the solvent was evaporated and the resulting yellow residue was dissolved

in water. Addition of excess NMe_4Cl in water gave a precipitate. The solid was filtered, washed with (50 mL × 3), and dried *in vacuo*, which afforded a tetramethylammonium salt of *nido*-**1** as a white powder (63 mg, 82%). Single crystals suitable for X-ray diffraction study were grown from vapor diffusion of Et_2O into a MeCN solution. ^{1}H NMR (acetone-d_6): δ 7.56 (s, 1H), 7.11–7.05 (m, 2H), 6.81 (s, 4H), 3.46 (s, 12H), 3.5–1.5 (br, 9H, B–*H*), 2.50 (s, 3H), 2.28 (s, 6H), 1.97 (s, 12H), 1.69 (s, 1H, C_{Cb}–*H*), −2.55 (br s, 1H, B–*H*–B). ^{13}C NMR (acetone-d_6): δ 145.5, 145.4, 141.2, 138.8, 138.4, 134.6, 129.8, 128.9, 56.0 (NMe_4), 23.8, 21.3, 20.9 (Cb–*C* and B–C_{Ar} signals were not observed). ^{11}B NMR (acetone-d_6): δ 77.9 (br s), −8.3 (1B), −9.7 (1B), −13.0 (1B), −15.5 (1B), −18.1 (2B), −22.9 (1B), −32.4 (1B), −35.2 (1B). Anal. Calcd for $C_{31}H_{51}B_{10}N$: C, 68.21; H, 9.42; N, 2.57%. Found: C, 68.07; H, 9.41; N, 2.91%.

1.3. X-ray crystallography

The crystallographic measurements of Me_4N salt of *nido*-**1** were performed on a Bruker SMART Apex II CCD area detector diffractometer with a graphite-monochromated Mo-Kα radiation (λ = 0.71073 Å) at 100(2) K. The Olex^2 program[1] was used for solving and refinement of the crystal structure. The positions of all non-hydrogen atoms were refined with anisotropic displacement factors. All hydrogen atoms were placed using a riding model, and their positions were constrained relative to their parent atoms. The selected bond lengths and angles are given in Table S1. Full details of the structure determinations have been deposited as a cif with the Cambridge Crystallographic Data Centre under CCDC deposition number 1996549. The data can be obtained free of charge via www.ccdc.cam.ac.uk/data_request/cif.

1.4. Cyclic voltammetry

Cyclic voltammetry measurements were carried out in DMF (1×10^{-3} M) with a three-electrode cell configuration comprising platinum working and counter electrodes and an $Ag/AgNO_3$ (0.01 M in CH_3CN) reference electrode at room temperature. Tetra-*n*-butylammonium hexafluorophosphate (0.1 M) was used as the supporting electrolyte. The redox potentials were recorded at a scan rate of 100–200 mV s^{-1} and are reported against the ferrocene/ferrocenium (Fc/Fc^+) redox couple. The electrochemical oxidation (E_{onset}) and reduction ($E_{1/2}$) were used for the determination of the HOMO and LUMO energy levels, respectively.

1.5. Photophysical measurements

UV/Vis absorption and photoluminescence (PL) spectra were recorded on a Varian Cary 100 and FS5 spectrophotometer, respectively. Solution PL spectra were obtained from oxygen-free and air-saturated

tetrahydrofuran (THF) solutions. The thin film samples were prepared by spin-coating of the THF solutions of PMMA matrices doped with compounds on quartz plates. Photoluminescence quantum yields (PLQYs, Φ_{PL}) of all samples were measured on an absolute PL quantum yield spectrophotometer (Quantaurus-QY C11347-11, Hamamatsu Photonics) equipped with a 3.3 inch integrating sphere. Transient PL decay curves were recorded on a FS5 spectrophotometer (Edinburgh Instruments) using a time-correlated single-photon counting (TCSPC) mode (EPL-375 picosecond pulsed diode laser as a light source) or a multi-channel scaling (MCS) mode (microsecond Xenon flashlamp as a light source). Temperature-dependent PL decays were obtained with an OptistatDN^{TM} cryostat (Oxford Instruments).

1.6. Theoretical calculations

All calculations were performed using the Gaussian 09 program package.[2] The geometry optimization of ground states was computed with density functional theory (DFT) at the M062X/6-31g(d) levels,[3] and the energy minima were confirmed by the calculation with zero imaginary mode of vibrations. The calculated absorptions were obtained with the time-dependent density functional theory (TD-DFT) method taking the ground state optimized geometry as the starting geometry. The ground state optimized geometry was used for the investigation of the vertical excitation and singlet-triplet energy splitting (ΔE_{ST}). In order to investigate the methyl substitution effect on the rotational dependency of the TADF properties, relaxed potential energy surface and ΔE_{ST} calculations were performed at every fixed rotational angle of *nido*-carborane cage (10°). The overlap integral extents were computed using Multiwfn programs.[4]

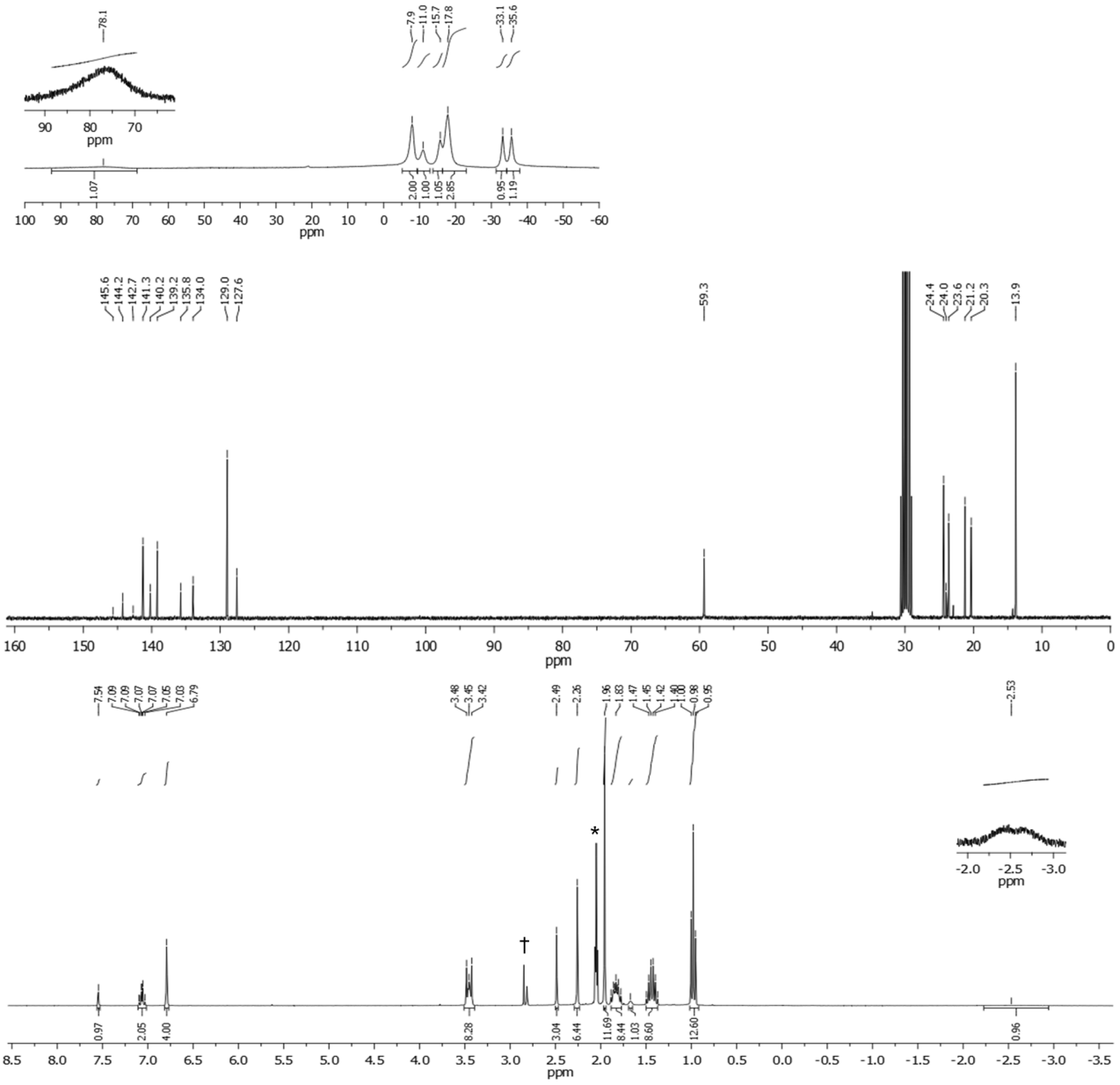

Figure S1. ^{11}B (top), ^{13}C (middle), and ^{1}H (bottom) NMR spectra of *nido*-**1** (∗ from residual solvent, † from H_2O in acetone-d_6).

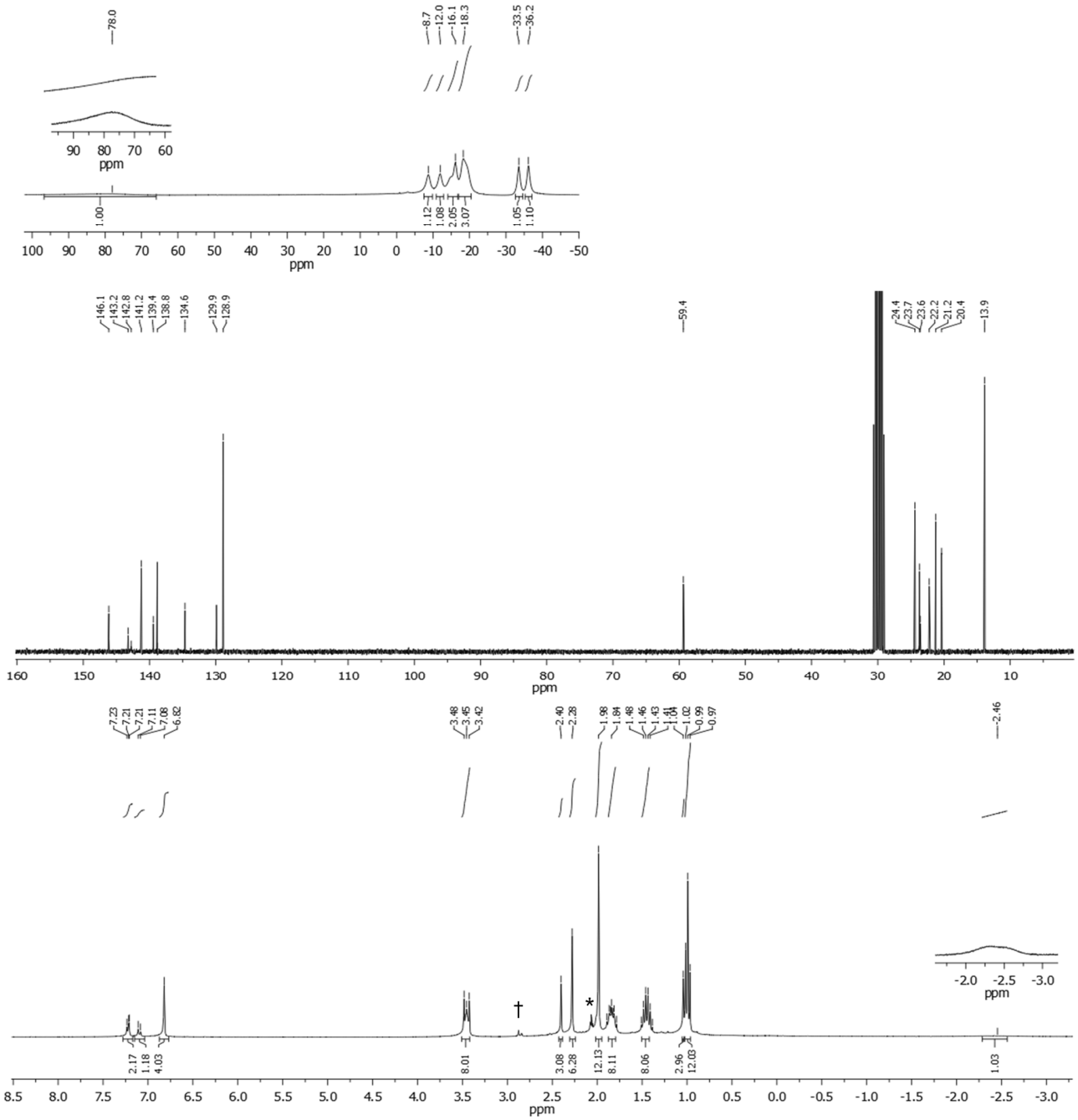

Figure S2. ^{11}B (top), ^{13}C (middle), and ^{1}H (bottom) NMR spectra of *nido*-**2** (∗ from residual solvent, † from H_2O in acetone-d_6).

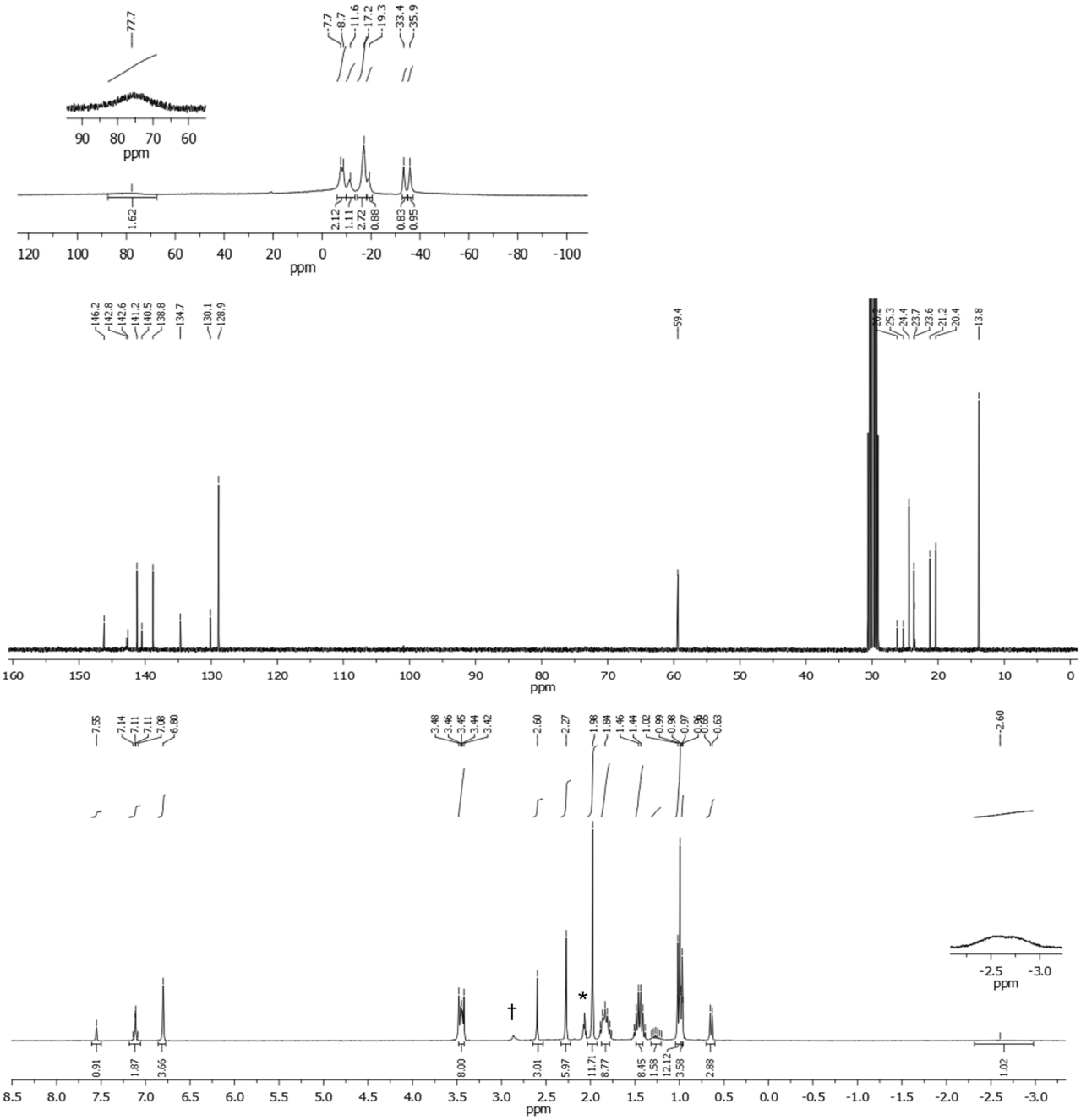

Figure S3. ^{11}B (top), ^{13}C (middle), and ^{1}H (bottom) NMR spectra of *nido*-**3** (∗ from residual solvent, † from H_2O in acetone-d_6).

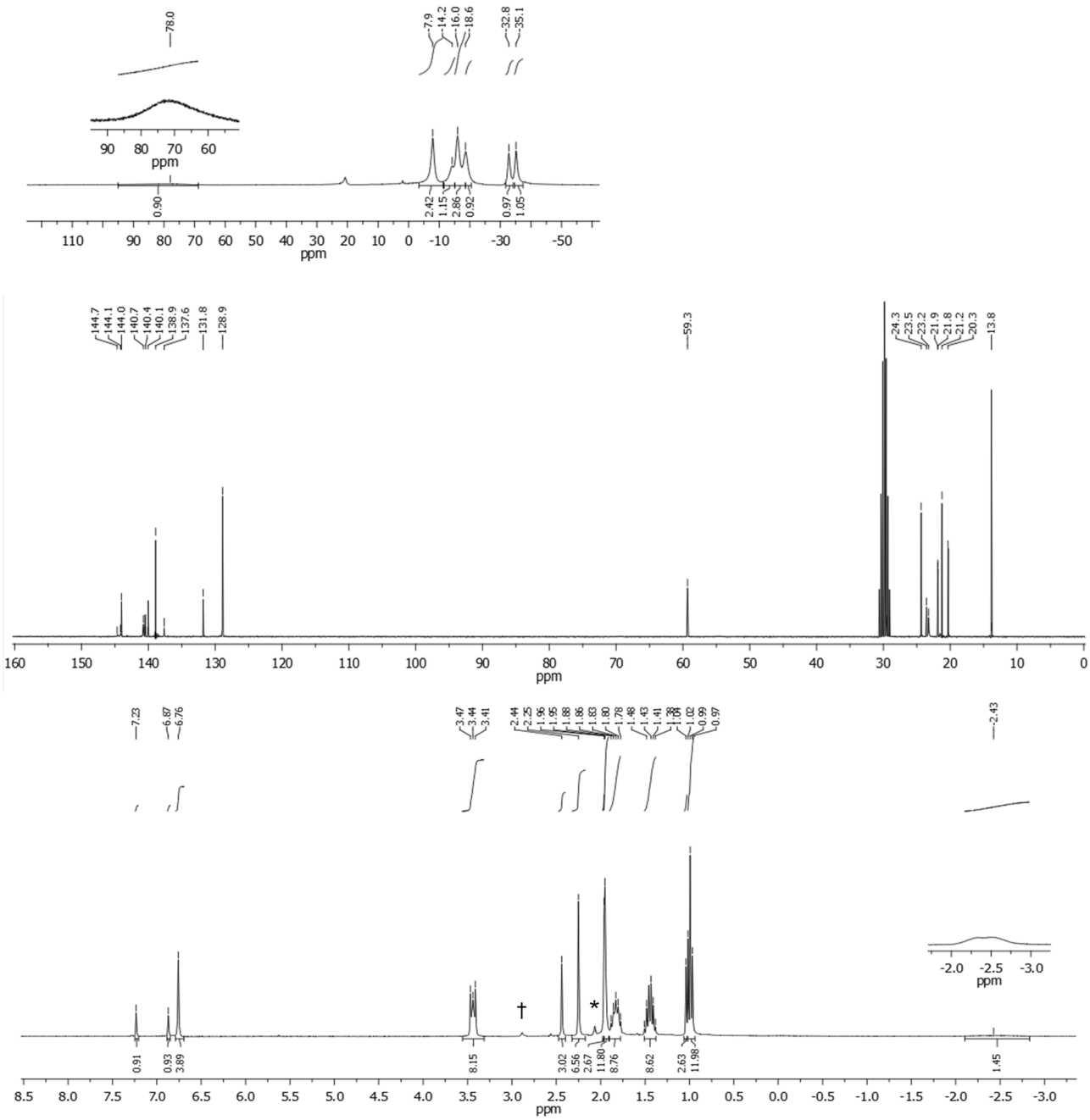

Figure S4. ^{11}B (top), ^{13}C (middle), and ^{1}H (bottom) NMR spectra of *nido*-**4** (∗ from residual solvent).

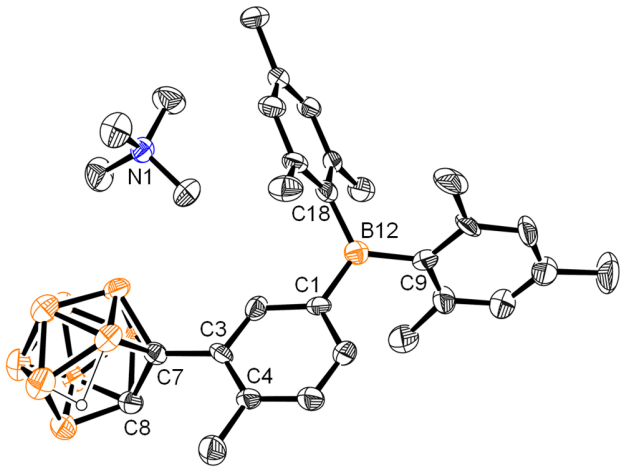

Figure S5. X-ray crystal structure of *nido*-**1** (40% thermal ellipsoids). H atoms are omitted for clarity.

Table S1. Selected bond lengths (Å) and angles (deg) for Me_4N salt of *nido*-**1**.

	nido-**1** (Me_4N salt)
Lengths	
B(12)–C(1)	1.570(10)
B(12)–C(9)	1.590(11)
B(12)–C(18)	1.570(11)
C(7)–C(8)	1.569(9)
Angles	
C(1)–B(12)–C(9)	120.3(7)
C(1)–B(12)–C(18)	119.4(6)
C(9)–B(12)–C(18)	120.1(7)

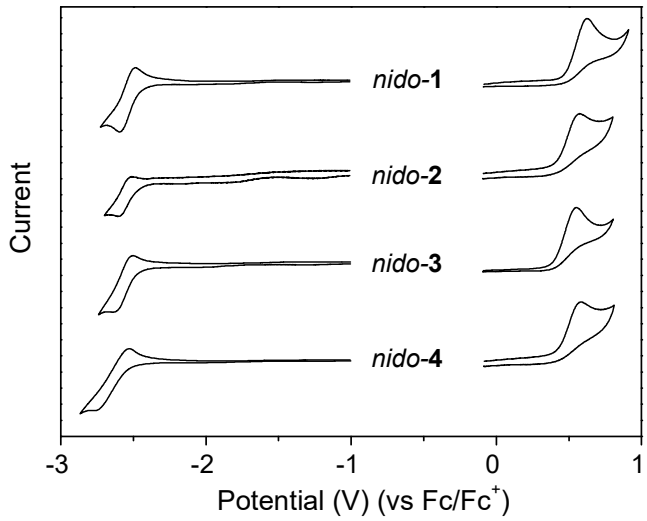

	E_{red} (V)	E_{ox} (V)	E_g (eV)
nido-**1**	−2.53	0.48	3.01
nido-**2**	−2.55	0.43	2.98
nido-**3**	−2.57	0.40	2.97
nido-**4**	−2.65	0.37	3.02

Figure S6. Cyclic voltammograms of *nido*-**1**–**4** showing electrochemical reduction (left, $E_{1/2}$) and oxidation (right, E_{onset}) (1.0×10^{-3} M in DMF, scan rate = 100–200 mV s^{-1}).

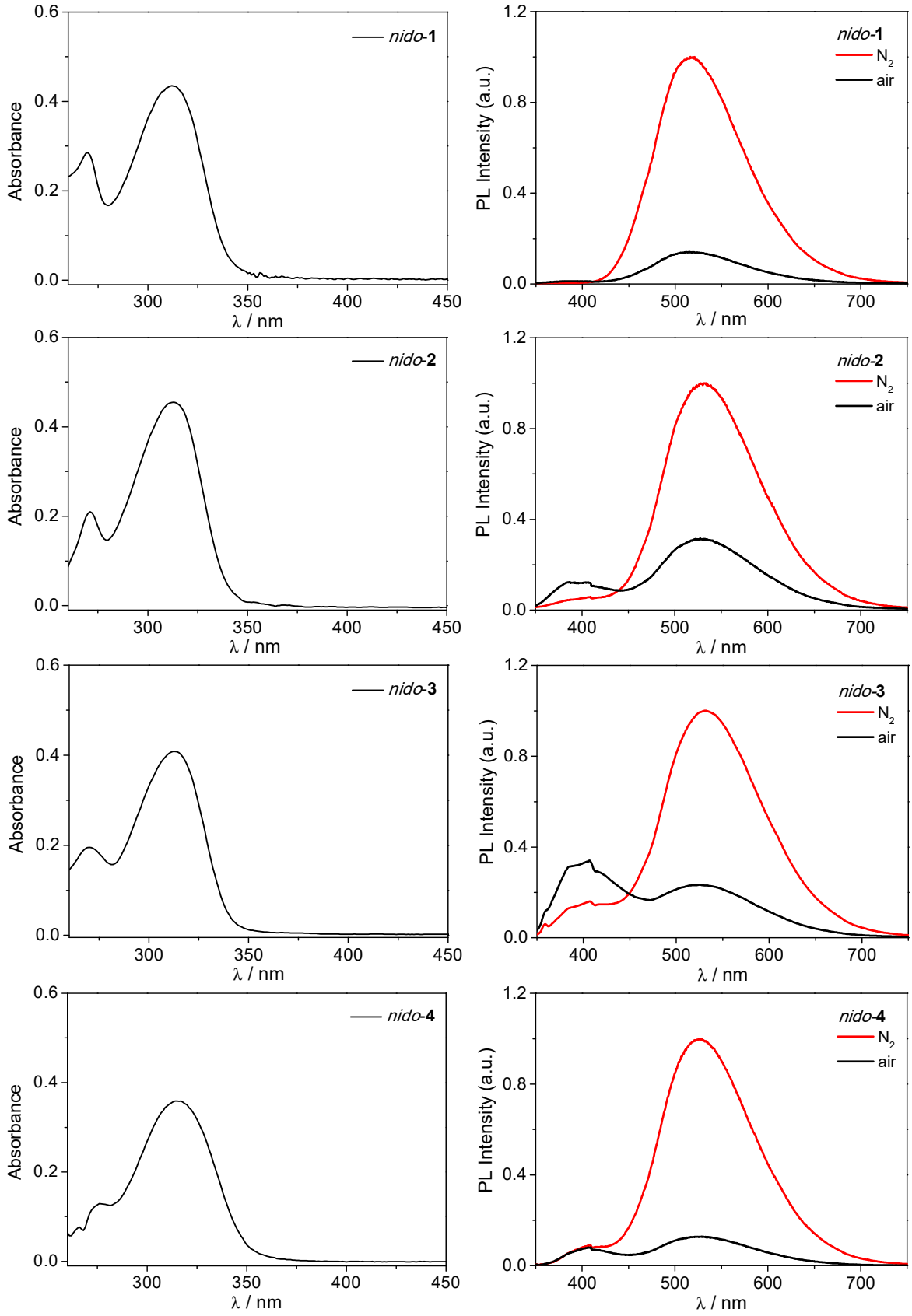

Figure S7. UV/Vis absorption (left) and PL spectra (right) of *nido*-**1**–**4** in oxygen-free (red line) and air-saturated (black line) THF (2.0×10^{-5} M) at 298 K.

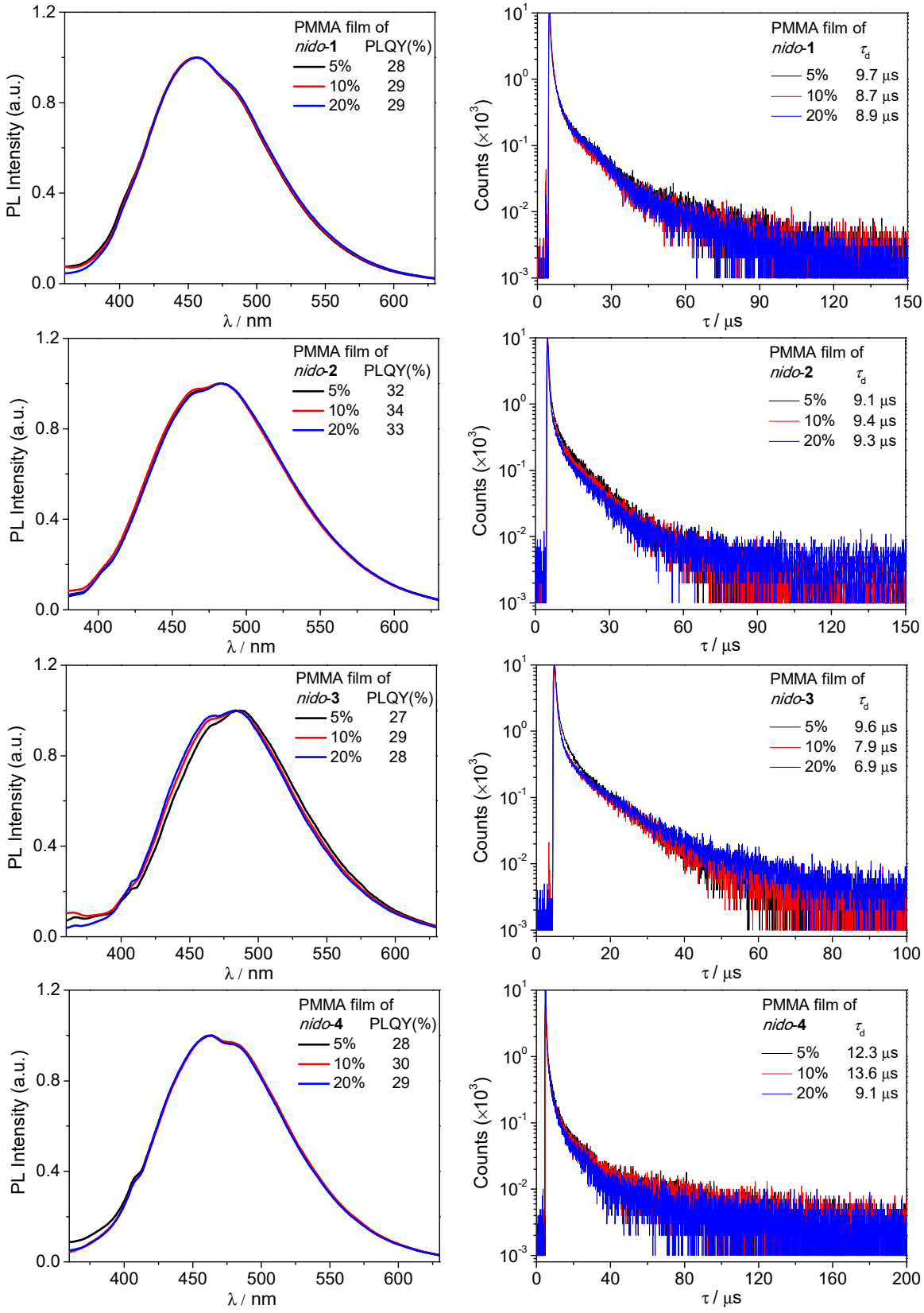

Figure S8. PL spectra (left) and transient PL decay curves (right) of the PMMA films doped with *nido*-**1**–**4** at different doping concentrations (5–20 wt%). λ_{exc} = 311 nm for *nido*-**1**; 312 nm for *nido*-**2** and -**3**; 320 nm for *nido*-**4**. PLQYs (%) and delayed lifetimes (τ_d) are provided.

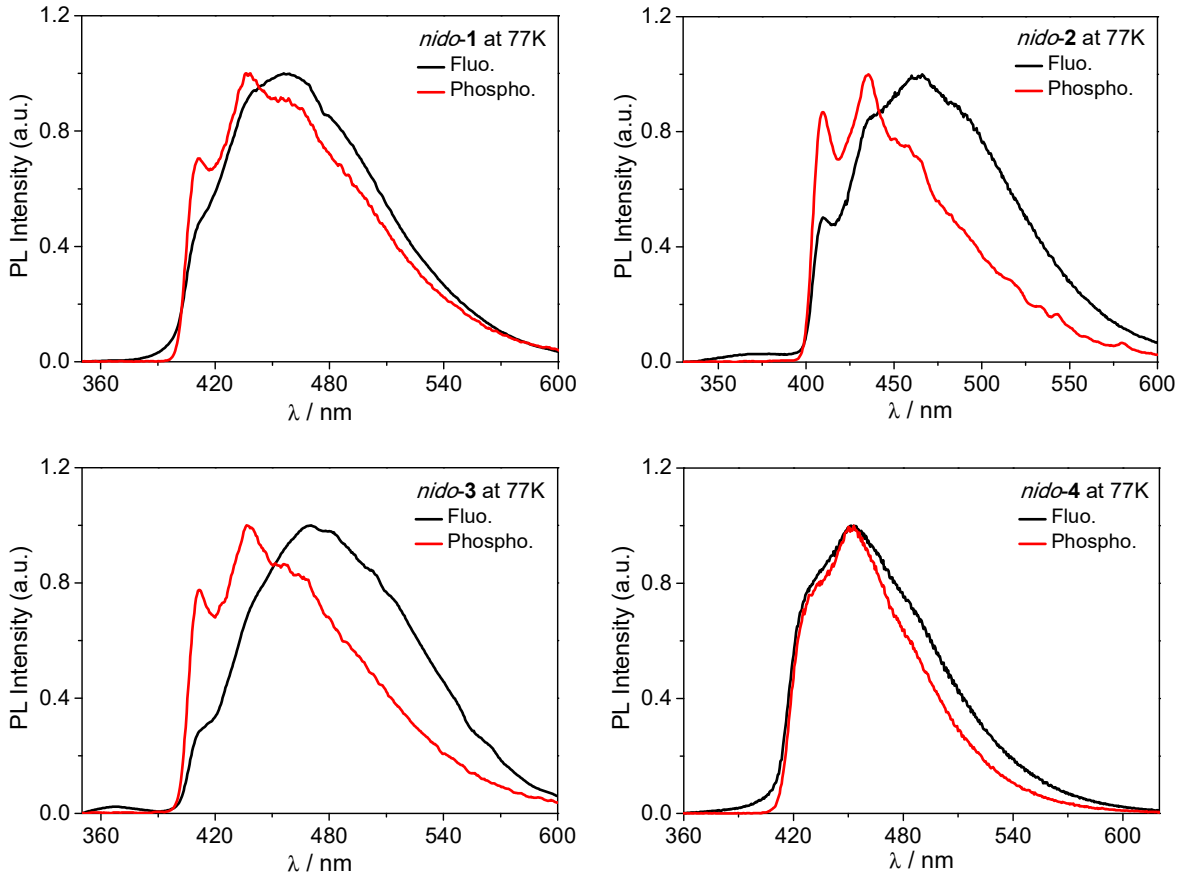

Figure S9. Fluorescence and phosphorescence (10 ms delay) spectra of *nido*-**1**–**4** in THF at 77 K. λ_{exc} = 316 nm for *nido*-**1**; 312 nm for *nido*-**2** and -**3**; 318 nm for *nido*-**4**.

Table S2. Rate constants for *nido*-**1**–**4** in THF.[a]

Compd	k_r (10^6 s^{-1})	k_p (10^7 s^{-1})	k_d (10^5 s^{-1})	$k_{nr,S}$ (10^6 s^{-1})	k_{ISC} (10^6 s^{-1})	k_{RISC} (10^5 s^{-1})
nido-**1**	1.47	1.01	1.03	4.66	3.92	1.69
nido-**2**	1.04	1.39	1.79	9.38	3.47	2.38
nido-**3**	1.05	1.42	2.08	10.6	2.55	2.54
nido-**4**	0.95	1.07	1.64	4.06	5.65	3.49

[a]Calculated using the reported method.[5] k_r, radiative decay rate constant ($S_1 \rightarrow S_0$); k_p, decay rate constant for prompt fluorescence; k_d, decay rate constant for delayed fluorescence; $k_{nr,S}$, nonradiative decay rate constant in the S_1 state; k_{ISC}, intersystem crossing (ISC) rate constant ($S_1 \rightarrow T_1$); k_{RISC}, reverse ISC rate constant ($T_1 \rightarrow S_1$).

2. Computational results

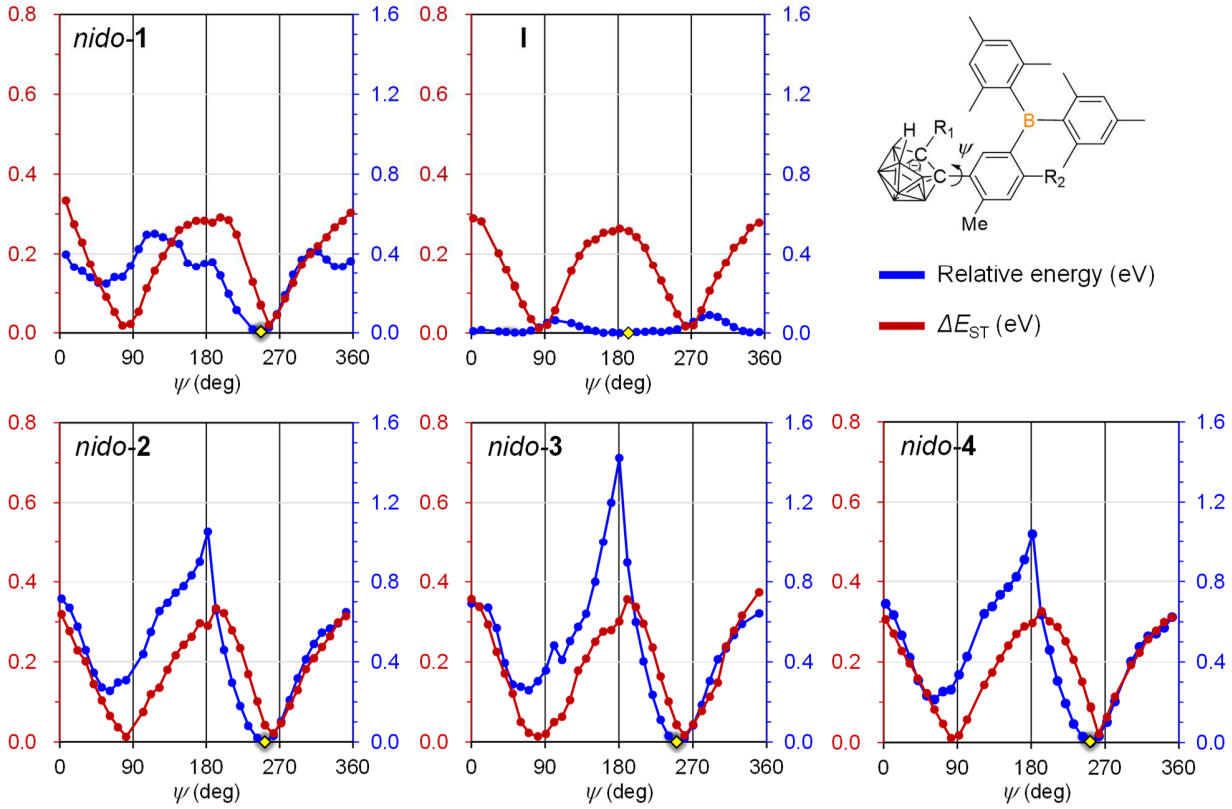

Figure S10. Calculated energy splitting between the S_1 and T_1 states (ΔE_{ST}) and relative energies of *nido*-**1**–**4** and reference **I** according to the rotation of the *nido*-carborane cage.

Table S3. The contribution (in %) of donor (*nido*-carborane) and acceptor ($PhBMes_2$) moieties to the frontier molecular orbitals and the overlap integral ($I_{H/L}$, in %) between HOMO and LUMO for *nido*-**1**–**4**.

	MO	Energy (eV)	Donor (*nido*-8-R-CB)	Acceptor ($PhBMes_2$)	$I_{H/L}$
nido-**1**	LUMO	1.28	0.31	99.68	9.92
	HOMO	−3.43	97.45	2.25	
nido-**2**	LUMO	1.27	0.37	99.63	9.40
	HOMO	−3.39	97.62	2.38	
nido-**3**	LUMO	1.26	0.46	99.54	9.10
	HOMO	−3.43	97.75	2.25	
nido-**4**	LUMO	1.24	0.33	99.66	8.99
	HOMO	−3.35	97.74	2.26	

Table S4. The calculated lowest-energy absorption wavelength (λ_{abs}, in nm) and the corresponding oscillator strength (f) for *nido*-**1**–**4**.

	λ_{abs}	f	major contribution
nido-**1**	367.3	0.0008	HOMO→LUMO (95%)
nido-**2**	372.6	0.0003	HOMO→LUMO (95%)
nido-**3**	370.6	0.0005	HOMO→LUMO (96%)
nido-**4**	377.9	0.0007	HOMO→LUMO (95%)

Table S5. Calculated HOMO–LUMO gap (E_g), the energies of the lowest singlet and triplet excited states (E_{S1} and E_{T1}), energy splitting between the S_1 and T_1 states (ΔE_{ST}), and torsion angle (ψ = C_{Cb}–C_{Cb}–C_{Ph}–C_{Ph}). Energy is in eV and angle is in degree (°).

	E_g	E_{S1}	E_{T1}	ΔE_{ST}	ψ
nido-**1**	4.71	3.38	3.30	0.071	68.9
nido-**2**	4.66	3.33	3.29	0.041	73.3
nido-**3**	4.69	3.35	3.32	0.026	75.9
nido-**4**	4.59	3.28	3.22	0.061	75.8

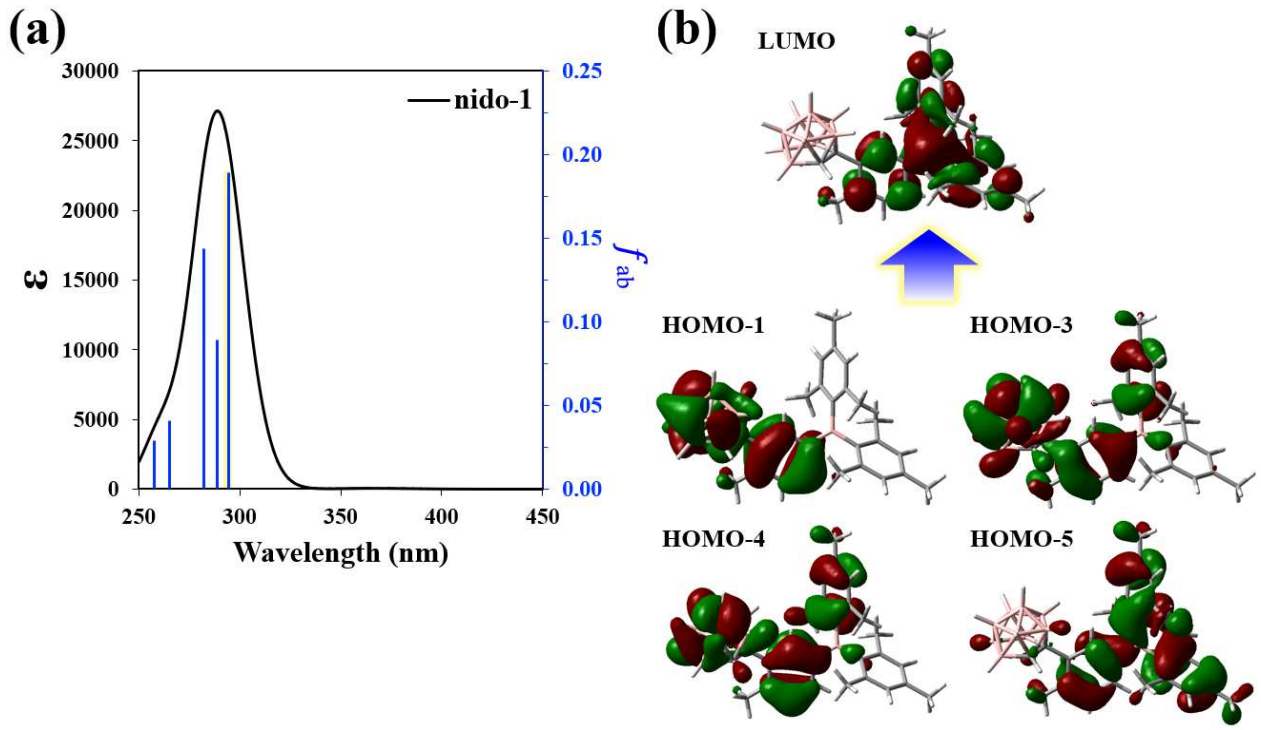

Figure S11. (a) Simulated UV/Vis absorption spectrum of *nido*-**1** (**ε** is molar absorption coefficient) and (b) MOs involved in the transition of the first non-zero oscillator strength (S_2).

Table S6. Computed absorption wavelengths (λ_{calc} in nm) and corresponding oscillator strength (f_{ab}) for *nido*-**1** from TD-M062X calculations using the M062X geometries at the ground (S_0) fully optimized geometry.

nido-**1**			
state	$\lambda_{calc.}$/nm	f_{abs}	major contribution
S_1	367.3	0.0008	HOMO→LUMO (95%)
S_2	294.3	0.1892	HOMO-5→LUMO (15%)
			HOMO-4→LUMO (30%)
			HOMO-3→LUMO (31%)
			HOMO-1→LUMO (12%)
S_3	288.6	0.0894	HOMO-5→LUMO (31%)
			HOMO-1→LUMO (44%)
S_4	282.1	0.1437	HOMO-5→LUMO (36%)
			HOMO-4→LUMO (21%)
			HOMO-1→LUMO (16%)
S_5	265.2	0.0408	HOMO-6→LUMO (82%)
S_6	257.6	0.0291	HOMO→LUMO+3 (27%)
			HOMO→LUMO+5 (62%)

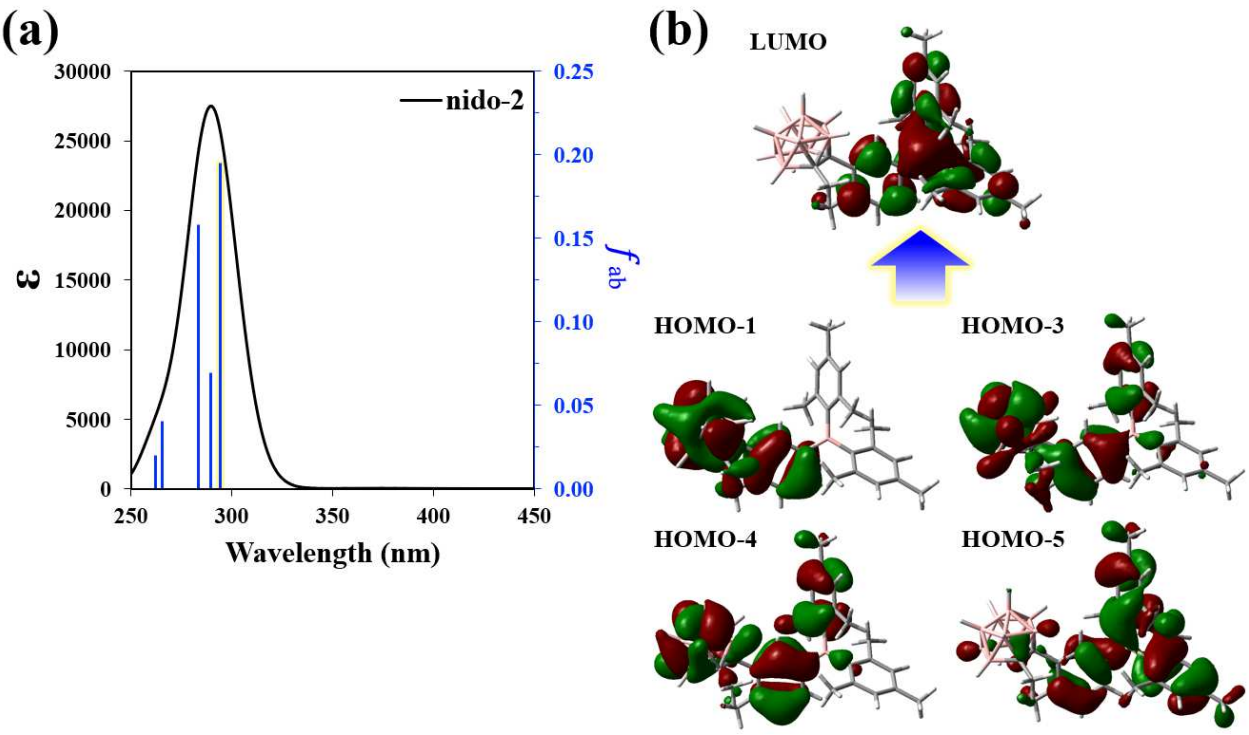

Figure S12. (a) Simulated UV/Vis absorption spectrum of *nido*-**2** (**ε** is molar absorption coefficient) and (b) MOs involved in the transition of the first non-zero oscillator strength (S_2).

Table S7. Computed absorption wavelengths (λ_{calc} in nm) and corresponding oscillator strength (f_{ab}) for *nido*-**2** from TD-M062X calculations using the M062X geometries at the ground (S_0) fully optimized geometry.

nido-**2**			
state	$\lambda_{calc.}$/nm	f_{abs}	major contribution
S_1	372.6	0.0003	HOMO→LUMO (95%)
S_2	294.4	0.1952	HOMO-5→LUMO (15%)
			HOMO-4→LUMO (29%)
			HOMO-3→LUMO (31%)
			HOMO-1→LUMO (11%)
S_3	289.7	0.0697	HOMO-5→LUMO (29%)
			HOMO-1→LUMO (39%)
S_4	283.2	0.1579	HOMO-5→LUMO (38%)
			HOMO-4→LUMO (19%)
			HOMO-1→LUMO (14%)
S_5	265.3	0.0408	HOMO-6→LUMO (81%)
S_6	261.9	0.0200	HOMO→LUMO+3 (29%)
			HOMO→LUMO+5 (62%)

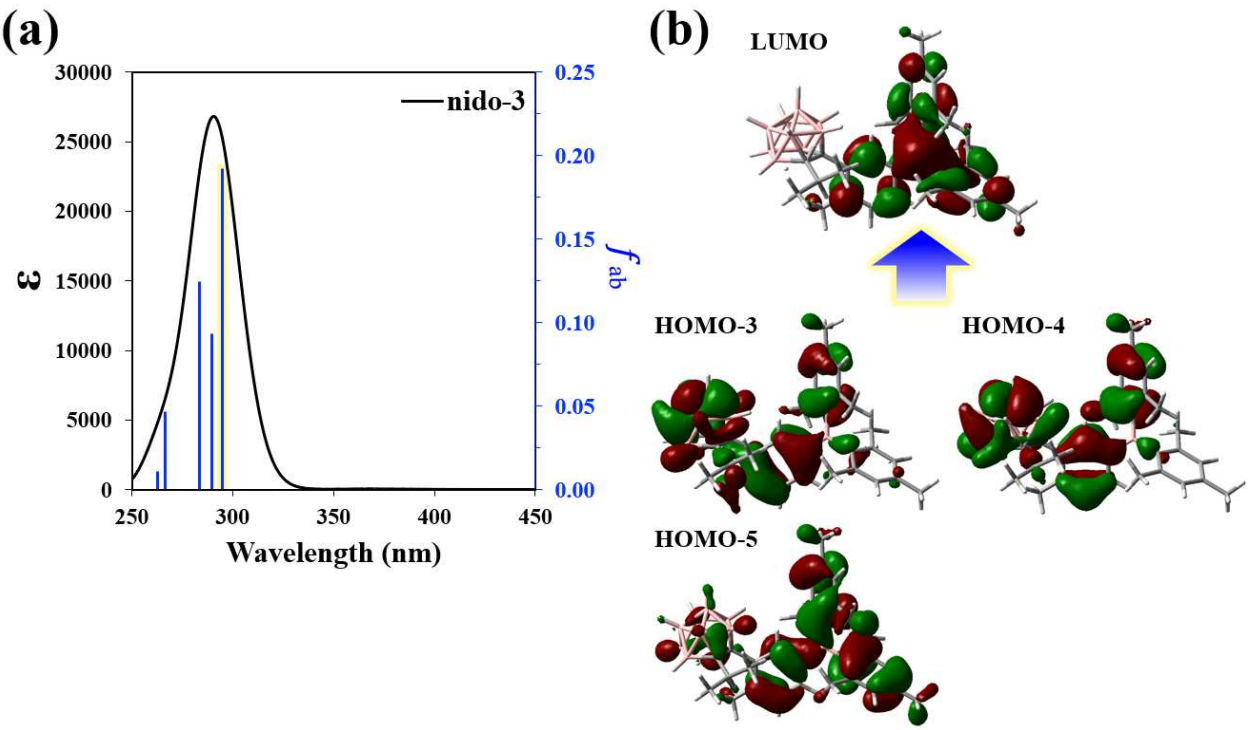

Figure S13. (a) Simulated UV/Vis absorption spectrum of *nido*-**3** (**ε** is molar absorption coefficient) and (b) MOs involved in the transition of the first non-zero oscillator strength (S_2).

Table S8. Computed absorption wavelengths (λ_{calc} in nm) and corresponding oscillator strength (f_{ab}) for *nido*-**3** from TD-M062X calculations using the M062X geometries at the ground (S_0) fully optimized geometry.

nido-**3**			
state	$\lambda_{calc.}$/nm	f_{abs}	major contribution
S_1	370.6	0.0005	HOMO→LUMO (96%)
S_2	295.0	0.1919	HOMO-5→LUMO (12%)
			HOMO-4→LUMO (30%)
			HOMO-3→LUMO (38%)
S_3	289.8	0.0932	HOMO-5→LUMO (32%)
			HOMO-1→LUMO (35%)
S_4	283.3	0.1243	HOMO-5→LUMO (36%)
			HOMO-4→LUMO (13%)
			HOMO-1→LUMO (20%)
S_5	266.5	0.0467	HOMO-6→LUMO (78%)
S_6	262.5	0.0111	HOMO→LUMO+3 (39%)
			HOMO→LUMO+5 (50%)

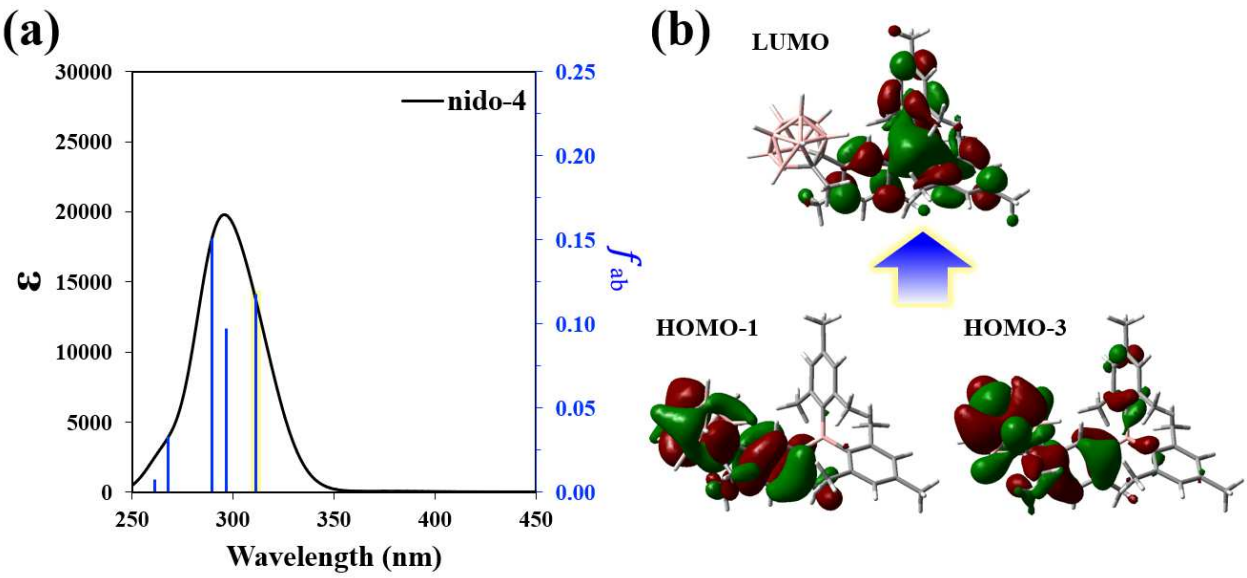

Figure S14. (a) Simulated UV/Vis absorption spectrum of *nido*-**4** (**ε** is molar absorption coefficient) and (b) MOs involved in the transition of the first non-zero oscillator strength (S_2).

Table S9. Computed absorption wavelengths (λ_{calc} in nm) and corresponding oscillator strength (f_{ab}) for *nido*-**4** from TD-M062X calculations using the M062X geometries at the ground (S_0) fully optimized geometry.

nido-**4**			
state	λ_{calc}/ nm	f_{ab}	major contribution
S_1	377.9	0.0007	HOMO→LUMO (95%)
S_2	311.4	0.1178	HOMO-3→LUMO (14%)
			HOMO-1→LUMO (59%)
S_3	296.6	0.0972	HOMO-5→LUMO (65%)
			HOMO-4→LUMO (19%)
S_4	289.4	0.1509	HOMO-5→LUMO (18%)
			HOMO-4→LUMO (37%)
			HOMO-1→LUMO (14%)
S_5	267.9	0.0332	HOMO-7→LUMO (82%)
S_6	261.1	0.0078	HOMO→LUMO+3 (14%)
			HOMO→LUMO+5 (52%)

3. References

1. L. J. Bourhis, O. V. D., R. J. Gildea, J. A. K. Howard and H. Puschmann. The anatomy of a comprehensive constrained, restrained refinement program for the modern computing environment - Olex2 dissected. *Acta Crystallogr. A* **2015**, *71*, 59-75.

2. M. J. Frisch, G. W. Trucks, H. B. Schlegel, G. E. Scuseria, M. A. Robb, J. R. Cheeseman, G. Scalmani, V. Barone, B. Mennucci, G. A. Petersson, H. Nakatsuji, M. Caricato, X. Li, H. P. Hratchian, A. F. Izmaylov, J. Bloino, G. Zheng, J. L. Sonnenberg, M. Hada, M. Ehara, K. Toyota, R. Fukuda, J. Hasegawa, M. Ishida, T. Nakajima, Y. Honda, O. Kitao, H. Nakai, T. Vreven, J. A. Montgomery, Jr., J. E. Peralta, F. Ogliaro, M. Bearpark, J. J. Heyd, E. Brothers, K. N. Kudin, V. N. Staroverov, T. Keith, R. Kobayashi, J. Normand, K. Raghavachari, A. Rendell, J. C. Burant, S. S. Iyengar, J. Tomasi, M. Cossi, N. Rega, J. M. Millam, M. Klene, J. E. Knox, J. B. Cross, V. Bakken, C. Adamo, J. Jaramillo, R. Gomperts, R. E. Stratmann, O. Yazyev, A. J. Austin, R. Cammi, C. Pomelli, J. W. Ochterski, R. L. Martin, K. Morokuma, V. G. Zakrzewski, G. A. Voth, P. Salvador, J. J. Dannenberg, S. Dapprich, A. D. Daniels, O. Farkas, J. B. Foresman, J. V. Ortiz, J. Cioslowski, and D. J. Fox , *Gaussian 09, Revision E.01*.; Gaussian, Inc.: Wallingford, CT, 2013.

3. Y. Zhao, D. G. Truhlar, *J. Phys. Chem. A* **2006**, *110*, 13126-13130.

4. T. Lu, F. Chen, *J. Comput. Chem*. **2012**, *33*, 580-592.

5. K.-C. Pan, S.-W. Li, Y.-Y. Ho, Y.-J. Shiu, W.-L. Tsai, M. Jiao, W.-K. Lee, C.-C. Wu, C.-L. Chung, T. Chatterjee, Y.-S. Li, K.-T. Wong, H.-C. Hu, C.-C. Chen and M.-T. Lee, *Adv. Funct. Mater.* **2016**, *26*, 7560-7571.